



Staron, L. H., & Phillips, J. C. (2016). How large grains increase bulk friction in bi-disperse granular chute flows. *Computational Particle Mechanics*, 3(3), 367-372. <https://doi.org/10.1007/s40571-015-0068-1>

Peer reviewed version

License (if available):  
Unspecified

Link to published version (if available):  
[10.1007/s40571-015-0068-1](https://doi.org/10.1007/s40571-015-0068-1)

[Link to publication record in Explore Bristol Research](#)  
PDF-document

This is the author accepted manuscript (AAM). The final published version (version of record) is available online at Springer via <http://dx.doi.org/10.1007/s40571-015-0068-1>. Please refer to any applicable terms of use of the publisher.

## University of Bristol - Explore Bristol Research

### General rights

This document is made available in accordance with publisher policies. Please cite only the published version using the reference above. Full terms of use are available:  
<http://www.bristol.ac.uk/red/research-policy/pure/user-guides/ebr-terms/>

# Discrete simulations of size segregating granular chute flows

Lydie Staron · Jeremy C. Phillips

Received: date / Accepted: date

**Abstract** Discrete numerical simulations are performed to study size segregation in granular flows. The stress state is measured accurately within the two phases of grains. It reveals a greater shear strength in the phase of larger grains, while suggesting that partial pressure scalings are dominated by the flow composition. Considering long flow durations made possible by periodic boundary conditions, we characterize the final segregated state by its steady-state mean velocity. We show that bi-disperse granular flows still obey the well-known Bagnold scaling, and that their velocity is at leading order controlled by the length scale set by the grain sizes and the flow composition.

**Keywords** Size segregation · Pressure scaling · Contact Dynamics

## 1 Introduction

Size segregation occurs when a granular bed made of grains of different sizes is submitted to shear or shaking under gravity during a sufficiently long lapse of time: larger grains rise at the top while smaller grains are trapped at the bottom. This behavior is robust; everyone has witnessed it either in nature - sorting of sand or pebbles in dunes or rivers - or simply at home in one's cereal box for instance [30, 7, 8, 33]. Since raw material often comes in the shape of grains, size segregation is a constant concern for many industries: food industry, pharmacology, civil engineering, and for any other processes handling

---

L. Staron

1- Sorbonne Univ, UPMC Univ Paris 06, UMR 7190, Inst Jean Le Rond d'Alembert, F-75005, Paris, France

2- CNRS, UMR 7190, Inst Jean Le Rond d'Alembert, F-75005, Paris, France

3- School of Earth Sciences, University of Bristol, United Kingdom

E-mail: lydie.staron@upmc.fr

J. C. Phillips

School of Earth Sciences, University of Bristol, United Kingdom

grains [3].

Size segregation may at first appear a simple mechanism. Indeed, the fact that smaller grains have a higher probability to fill in the gaps opening in the granular bed as a result of shear or shakes (as described in [34]) seems enough to account for the final sorting of the grains. It is however a very complex challenge to modeling. Obvious questions are: what are the typical time scales? when does the segregation saturates and why? what are the feedbacks between segregation and flow dynamics? is there a single mechanism at play or various ones depending on the grain sizes involved? and finally, how to translate this or these mechanisms into a dynamical expression that may fit into a continuum description?

Numerous works have addressed these issues using different approaches. Experiments are the privileged tool to evidence intricate phenomenologies involving different grain sizes, in free surface flows [2, 28, 12, 27, 42, 5], shear cells [10] or in vibrating beds [21, 35, 9]. Precise measurements in granular system are however uneasy, and only extremely well controlled experiments may lead to a quantitative picture of the physics at play during segregation [10, 16, 17]. For this reason, discrete numerical simulation has proven a helpful tool to analyze the local mechanisms at play during segregation and to understand the structure of poly-disperse granular systems [31, 44, 6, 23, 38, 36, 18]. They are also a practical mean to inform continuum modeling [13, 14, 25, 38, 20].

In this contribution, we apply discrete simulations to explore various features of size segregating granular chute flows: the stress state, the mean flow velocity and the influence of geometrical factors. Doing so, we underline the fact that taking into account the granular nature of the flow is crucial to understand the influence of segregation on its behavior. The numerical technics used - the contact dynamics - is described in section 2 together with the flow configuration adopted for our study. The general behavior is reported in section 3. Pressure scalings and the stress state are then analyzed in section 4. Finally, section 5 stresses how the length scale introduced by the grain size plays a central role in setting the flow velocity.

## 2 Discrete simulations of bi-disperse granular flows

### 2.1 The contact dynamics method

This numerical experiment was performed using the now well-known Contact Dynamics algorithm [19, 26]. An important advantage of this algorithm is its reliability to mimic the behavior of perfectly rigid grains in a multi-contact environment typical for dense flow regimes. Its efficiency for exploring poly-disperse granular packings is demonstrated was [41]. It is not our intention in this contribution to present the Contact Dynamics in its full complexity. We refer the reader to [?] for details on this aspect.

While at contact, grains interact through a friction force that allow for slip

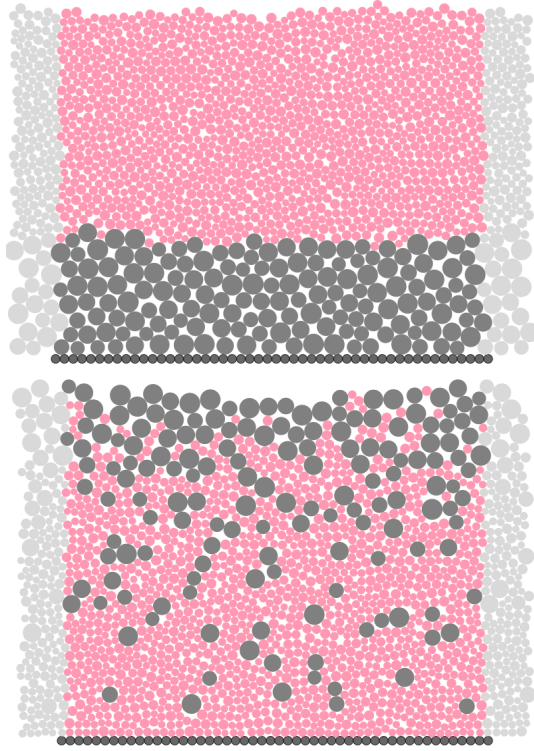


**Fig. 1** Bi-disperse granular flow with a volume fraction of large beads  $\xi = 0.34$ , in its initial state and after steady-state is reached and segregation occurred (slope  $\theta = 18^\circ$ ).

motion when the tangential force  $T$  reaches the frictional threshold set by the coefficient of friction  $\mu$  and the compressive force  $N$ . In dense packings (as those simulated for this study), friction is very efficient at dissipating energy. In the following, the friction coefficient is set to  $\mu = 0.5$  for all contacts, irrespective of the size of the grains involved.

Another efficient way by which granular flows dissipate their energy is through non-elastic collisions: the coefficient of restitution  $e$  is smaller than one so that grains bounce back with less momentum. We chose  $e = 0.25$  for all contacts.

## 2.2 The numerical simulations

The configuration chosen to study segregation is a two-dimensional granular chute flow of slope  $\theta$ , as described in [36]. Two grain sizes are considered. The larger grains - placed initially at the bottom of the granular layer - rise to the surface as the flow develops, as illustrated in Figure 1. The periodic boundary conditions in the flow direction allows for infinite flow durations. This typical

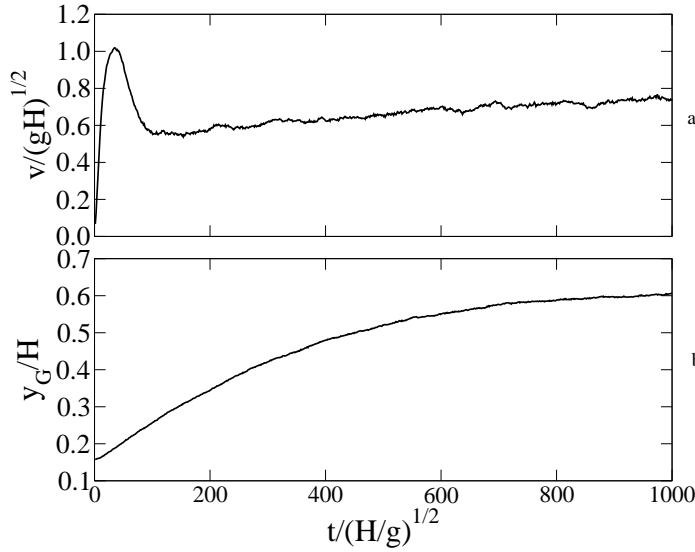


**Fig. 2** (a) Mean flow velocity  $v$  (normalized by  $\sqrt{gH}$ ) and (b) Position of the center of mass of large grains  $y_G$  (normalized by  $H$ ) as a function of time (normalized by  $\sqrt{H/g}$ ) for  $\xi = 0.34$  and  $\theta = 18^\circ$ .

chute flow experiment is in its principle similar to those reported in [31,38, 23].

We denote  $d_L$  and  $d_S$  the mean diameter of large and small grains respectively, taken so that the size ratio is  $d_L/d_S = 2$ . The value of this ratio on the flow behavior is important: both the time scales of the segregation and the level of sorting (ie the saturation rate) are affected [31,10,38]. We do not investigate this aspect in the following. The choice  $d_L/d_S = 2$  is motivated by earlier studies showing that it does favor segregation. To prevent geometrical ordering, both large and small grains have diameters uniformly distributed around their mean value within a size interval of 40%.

The width of the simulation cell is  $50d_S$ . The bottom is made of a row of small grains. In the initial state, a layer of large grains is overlaid by a layer of small grains, both deposited by random rain under gravity (Figure 1, top). The volume fraction of large grains is denoted  $\xi$ , ie the ratio of the volume of large grains to the total volume of grains:  $\xi = V_L/(V_S + V_L)$ . The volume fraction of small grains is thus  $(1 - \xi)$ . The height of the granular bed in the initial state is kept constant:  $H \simeq 45d_S$ . Both the slope  $\theta$  and the volume fraction of large grains  $\xi$  are varied.

The numerical values used are:  $d_S = 5.10^{-3}\text{m}$ ,  $\rho = 1 \text{ kg.m}^{-2}$ ,  $g = 9.8 \text{ m.s}^{-2}$ .

### 3 General behavior

A typical time evolution is shown on Figure 2 for a slope  $\theta = 18^\circ$  and a volume fraction of large grains  $\xi = 0.34$  (like shown in Figure 1). The velocity (Figure 2-a) first undergoes a sharp increase quickly checked and followed by a deceleration phase; it then slowly evolves towards its steady state value. The existence of the initial peak is related to two independent facts. First, as segregation proceeds, the bottom condition characterized by the size of the grains involved changes from the favorable large-on-small configuration to the less favorable small-on-small configuration. This induces a change in the slip velocity which suddenly drops. Then, the vertical motion of the grains (upwards for the large and downwards for the small) dissipate energy through what can be described as similar to a drag [45,13,16,36]: the energetic cost of this is certainly visible in the deceleration phase. Interestingly, it seems to be significant in amplitude only in the early stage, during what may be called the initial squeeze expulsion phase (after [34]). After this initial phase, the evolution of the flow becomes smooth. For the same simulation, the vertical position of the center of mass of the large grains  $y_G$  is computed and plotted in Figure 2-b. We observe the regular rise following an exponential dependence, as discussed in details in [36].

From these graphs, segregation seems a relatively slow process. Here, the fact that the configuration is bi-dimensional is crucial. Clearly, geometrical rearrangements are much more difficult in 2D than in 3D, and the probability of gaps opening in the neighborhood of a given grain are significantly diminished by suppressing one dimension.

### 4 On the stress state

Segregation can be easily understood from a geometrical point of view, originally described by Savage and Lun [34] as the *percolation* of the smaller grains through the network of larger ones, or *random fluctuating sieve*. It renders the fact that at any instant, voids open randomly in the sheared flow, with the probability to find a void where small particles can fall in being greater than the probability to find a void where larger particles can fall in. However, understanding segregation in terms of a mechanical process is more challenging. It was only recently that a lift force was effectively measured in a granular packing, and the generalization to a rapid flow as studied in this paper is not straightforward [17]. A fruitful hypothesis was nevertheless proposed by Gray and Thornton [13] that allows for efficient continuum modeling of segregation in 3D configurations [20]: that smaller grains are screened from the mean pressure by the network of large grains. This however has to be ascertained from direct analysis of granular flows.

Using the micro-mechanical definition of the stress tensor [32]:

$$\boldsymbol{\sigma} = \frac{1}{V} \sum_N \mathbf{f} \otimes \mathbf{r}, \quad (1)$$

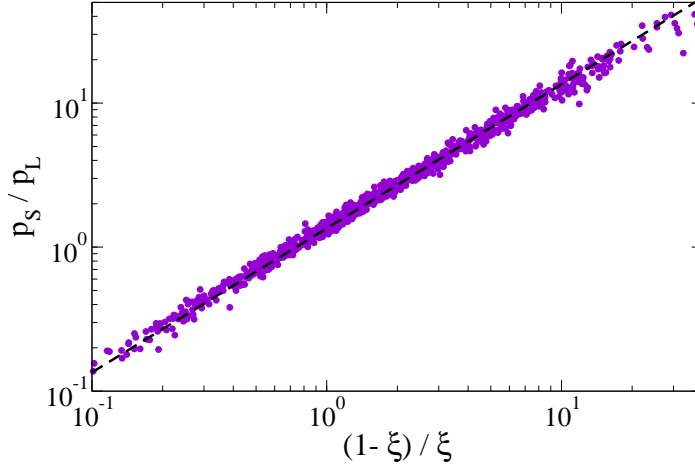


**Fig. 3** Ratio of the partial pressure of the phase of small grains  $p_S$  to the partial pressure of the phase of large grains  $p_L$  as a function of their relative volume fraction  $(1-\xi)/\xi$ , computed in the course of time at different depths in the flow. The dotted line shows  $y = 1.35x$ .

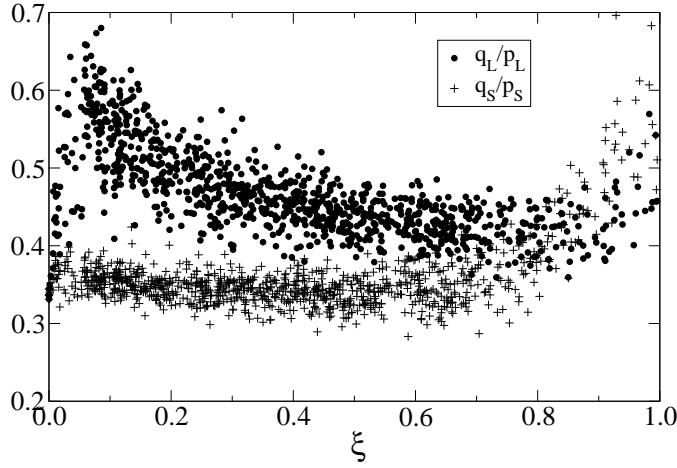


**Fig. 4** Ratio of the stress deviator to the pressure for the phase of large grains  $q_L/p_L$  and the phase of small grains  $q_S/p_S$  as a function of the volume fraction of large grains  $\xi$ , computed in the course of time at different depths in the flow.

where  $\mathbf{f}$  is the force transmitted at contact,  $\mathbf{r}$  is the vector joining the center of mass of the two grains in contact,  $\otimes$  is the dyadic product,  $N$  is the number of contacts over which the summation is made, and  $V$  is the volume over which the stress is computed, we separate the contributions of the large grains and of the small grains. Therefore, two stress tensors  $\boldsymbol{\sigma}_L$  and  $\boldsymbol{\sigma}_S$  are computed, respectively over the number of contacts involving at least one large grain and the number of contacts involving at least one small grain, and over the total volume  $V$  for both. We can thus compute the partial pressures associated to the phase of large grains  $p_L$  and the phase of small grains  $p_S$ . In a classical mixture, partial pressures are proportional to the volume fraction of the species considered. We thus expect  $p_L$  and  $p_S$  to be respectively proportional to  $\xi$  and  $(1 - \xi)$ . This is indeed what Figure 3 shows, for flows with different values of  $\xi$  ( $\xi = 0.16$ ,  $\xi = 0.34$ ,  $\xi = 0.5$  and  $\xi = 0.67$ ) and a slope  $\theta = 18^\circ$ , and  $p_L$  and  $p_S$  computed at different locations and different times. We observe that the ratio  $p_S/p_L$  shows a linear dependence on  $(1 - \xi)/\xi$ . In other words, the pressure distribution in the flow is largely dominated by the flow composition.

Nevertheless, additional insight is gained when comparing not only the partial pressures, but also the stress deviators  $q_L$  and  $q_S$  sustained by the two phases of grains. We form the ratios  $q_L/p_L$  and  $q_S/p_S$  for the same simulations described in Figure 3, at different locations in the flow and different times, and plot them against the local value of  $\xi$  (Figure 4). We observe that for most values of  $\xi$ , the shear strength of large grains exceeds the shear strength of smaller grains. This fact, observed by [41] for non-segregating polydisperse granular packings, seems to support the hypothesis by Gray and Thornton following which smaller grains are screened from the mean stress.

## 5 On the flow velocity

The general evolution displayed in Figure 2 for a flow with  $\xi = 0.34$  and a slope  $\theta = 18^\circ$  shows that the mean velocity tends towards a steady state value which characterizes the final segregated state. How this final steady state velocity, denoted  $V_{\text{inf}}$  in the following, depends on the flow composition is investigated by performing a series of simulations with  $\xi = 0, 0.16, 0.25, 0.34, 0.42, 0.50, 0.59, 0.67, 0.75, 0.83, 0.91$  and  $1$ . The results are shown in Figure 5 for a slope  $\theta = 18^\circ$ . We observe a regular decrease of  $V_{\text{inf}}$  with  $\xi$ , with the exception of the point corresponding to  $\xi = 1$ . In this last case indeed, as described in section 3, the bottom condition becomes "large-on-small" instead of the "small-on-small" configuration, thus changing the slip velocity in a way favorable to the flow. The general behavior however suggests that adding large grains to the flow slows it down. This decrease can be understood from a purely geometrical point of view. Indeed, in the granular chute flow geometry, the Bagnold scaling tells us that for a flow of height  $H$  with grains of diameter  $d$ , the steady-state flow velocity satisfies  $V_{\text{inf}}/\sqrt{gH} \propto H/d$  [1]. In a bi-disperse configuration, the diameter  $d$  must be replaced by a mean value that reflects the existence of two grains sizes. We thus need to introduce  $d_\xi = \xi d_L + (1 -$



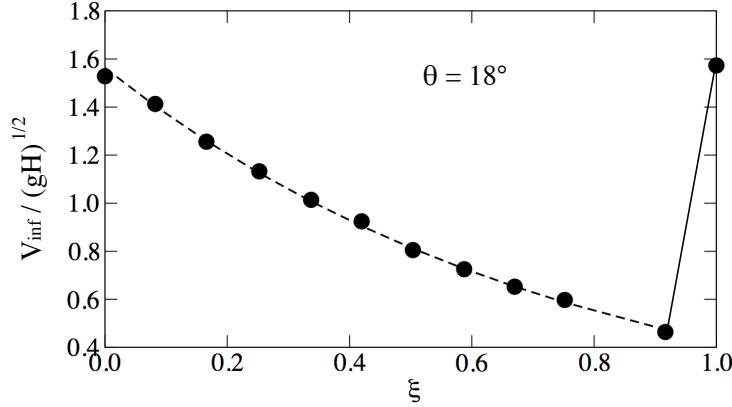


**Fig. 5** Ratio of the stress deviator to the pressure for the phase of large grains  $q_L/p_L$  and the phase of small grains  $q_S/p_S$  as a function of the volume fraction of large grains  $\xi$ , computed in the course of time at different depths in the flow.

$\xi$ )  $d_S$ . The Bagnold scaling now becomes  $V_{\text{inf}}/\sqrt{gH} \propto H/d_\xi$ , or equivalently,  $V_{\text{inf}}/\sqrt{gH} \propto 1/(1 + \xi)$ . This is this last dependence that we observe in Figure 5, materialized by the dotted line. Here, the dynamics of the flow cannot be understood independently of the length scale set by the grain sizes and the flow composition.

## 6 Conclusion

Discrete numerical simulations are a helpful tool to study the mechanisms driving size segregation in granular flows. The fact that contact properties are entirely controlled ensures that the phenomena observed result solely from grain size effects, and are not related to different surface properties or selective wear (as reported in [29, 40]). The stress state can be measured accurately within the two phases of grains. In the chute flows simulated in this contribution, the analysis of the stress state reveals a greater shear strength in the phase of larger grains, while suggesting that partial pressure scalings are dominated by the flow composition. Because long flow durations are made possible by periodic boundary conditions, we can characterize the final segregated state by its steady-state mean velocity. We can thus show that bi-disperse granular flows still obey the well-known Bagnold scaling [1], and that their steady-state velocity is at leading order controlled by the length scale set by the grain sizes and the flow composition.

**Acknowledgements** This work was supported by the FP7 European Grant IEF n°297843.

## References

1. Bagnold, R.G., *Proc. Roy. Soc. London Ser. A* **255**, 49 (1954)
2. G. Berton, R. Delannay, P. Richard, N. Taberlet, and A. Valance, *Phys. Rev. E* **68**, 051303 (2003)
3. J. Bridgewater, W. S. Foo, and D. J. Stephens, *Powder Technology* **41**, 147 - 158 (1985)
4. S. Deboeuf, E. Lajeunesse, O. Dauchot and B. Andreotti, *Phys. Rev. Lett.* **97**-15, 158303 (2005)
5. M. Degaetano, L. Lacaze and J. C. Phillips, *Euro. Phys. J. E* **36**-4, 1-9 (2013)
6. Yi Fan and K. M. Hill, *Phys. Rev. Lett.* **106** 218301 (2011)
7. G. Félix and N. Thomas, *Earth Planet. Sci. Lett.* **221**, 197-213 (2004).
8. P. Frey and Church M., *Science* **325**:1509-1510 (2009)
9. V. Garzo and F. V. Reyes, *Phys. Rev. E* **85**, 021308 (2012)
10. L. A. Golick and K. E. Daniels, *Phys. Rev. E* **80**, 042301 (2009)
11. C. Goujon, B. Dalloz-Dubrujeaud, and N. Thomas, *Euro. Phys. J. E* **11**, 147-157 (2003)
12. C. Goujon, B. Dalloz-Dubrujeaud, and N. Thomas, *Euro. Phys. J. E* **23**, 199-215 (2007)
13. J. M. N. T. Gray and A. R. Thornton, *Proc. R. Soc. A* **461**, 1447-1473 (2005)
14. J.M.N.T. Gray and V.A. Chugunov, *J. Fluid Mech.* **569**, 365-398 (2006)
15. Gray, J.M.N.T. and B. P. Kokelaar, *J. Fluid Mech.* **652**, 105-137 (2010)
16. F. Guillard, Y. Forterre and O. Pouliquen, *Phys. Rev. Lett.* **110**, 138303 (2013)
17. F. Guillard, Y. Forterre and O. Pouliquen, *Phys. Fluids* **26**, 043301 (2014)
18. K. M. Hill and D. S. Tan, *J. Fluid Mech.* **756**, 54-88 (2014)
19. M. Jean and J.-J. Moreau, In A. Curnier (ed), *Proc. of Contact Mech. Int. Symp.*, pp. 31-48. (1992)
20. C. G. Johnson, B. P. Kokelaar, R. M. Iverson, M. Logan, R. G. LaHusen, and J. M. N. T. Gray, *J. Geophys. Res.*, **117**, F01032 (2012)
21. A. Kudrolli, *Rep. Prog. Phys.* **67**, 209-247 (2004)
22. E. Linares-Guerrero, C. Goujon and R. Zenit, *J. Fluid Mech.* **593**, 475-504 (2007)
23. B. Marks, P. Rognon and I. Einav, *J. Fluid Mech.* **690**, pp. 499511 (2012)
24. L. B. H. May, L. A. Golick, K. C. Phillips, M. Shearer and K. E. Daniels, *Phys. Rev. E* **81**, 051301 (2010)
25. C. Meruane, A. Tamburrino and O. Roche, *Phys. Rev. E* **86**, 026311 (2012)
26. J.J. Moreau, *European Journal of Mechanics, A/Solids* **13**-4, p.93-114 (1994)
27. F. Moro, T. Faug, H. Bellot, F. Ousset, *Cold Regions Science and Technology* **62**, 55-66 (2010)
28. J. C. Phillips, A. J. Hogg, R. R. Kerswell and Thomas, N. H., *Earth and Planetary Sci. Lett.* **246**, 466 - 480 (2006)
29. O. Pouliquen, J. Delour, S. B. Savage, *Nature* **386**, 816-817 (1997) .
30. D. M. Powell, *Progress in Physical Geography* **22**-1, 1-32 (1998)
31. P. G. Rognon, J.-N. Roux, M. Naaïm, F. Chevoir, *Phys. of Fluids* **19**, 058101-1 (2007)
32. L. Rothenburg and R. J. Bathurst, *Geotechnique* **39**, 601 (1989)
33. P. J. Rowley, P. Kokelaar, M. Menzies and Waltham, D., *J. Sedimentary Res.* **81**, pp 874-884 (2011)
34. S. B. Savage and C. K. K. Lun, *J. Fluid Mech.*, **189**, 311-335 (1988)
35. M. Schröter, S. Ulrich, J. Kreft, J. B. Swift, and H. L. Swinney *Phys. Rev. E*, **74**, 011307 (2006)
36. L. Staron and J. C. Phillips, *Phys. Fluids* **26** (3), 033302 (2014)
37. G I. Tardos, M. I. Khan, and D. G. Schaeffer, *Phys. Fluids* **10**, 335 (1998)
38. A. R. Thornton, T. Weinhart, S. Luding, and Bokhove, O., *Int. J. of Modern Phys. C* **23**, 1240014 (2012)
39. A. Tripathi and D. V. Khakhar, *Phys. Fluids* **23**, 113302 (2011)
40. S. Ulrich, M. Schröter, and H. L. Swinney, *Phys. Rev. E* **76**, 042301 (2007)
41. C. Voivret, F. Radjai, J.-Y. Delenne, and M. S. El Youssofi, *Phys. Rev. Lett.* **102**, 178001 (2009)

- 
42. S. Wiederseiner, N. Andreini, G. Épely-Chauvin, G. Moser, M. Monnereau, J. M. N. T. Gray, and C. Ancey *Phys. Fluids* **23**, 013301 (2011)
  43. K. Wiegardt, *Annu. Rev. Fluid Mech.* **7**, pp. 89113 (1975)
  44. B. Yohannes and K. M. Hill, *Phys. Rev. E* **82**, 061301 (2010)
  45. O. Zik, J. Stavans and Y. Rabin, *Europhys. Lett.* **17** (4), pp. 315-319 (1992)
  46. I. Zuriguel, J.M.N.T. Gray, J. Peixinho and T. Mullin, *Phys. Rev. E* **73**, 061302 (2006)